**Bulletin of Mathematical Biology manuscript No.**
(will be inserted by the editor)

# Evolutionary stability of minimal mutation rates in an evo-epidemiological model

**Michael Birch** · **Benjamin M. Bolker**

Received: date / Accepted: date

**Abstract** We consider the evolution of mutation rate in a seasonally forced, deterministic, compartmental epidemiological model with a transmission-virulence trade-off. We model virulence as a quantitative genetic trait in a haploid population and mutation as continuous diffusion in the trait space. There is a mutation rate threshold above which the pathogen cannot invade a wholly susceptible population. The evolutionarily stable mutation rate is the one which drives the lowest *average* density, over the course of one forcing period, of susceptible individuals at steady state. In contrast with earlier eco-evolutionary models in which higher mutation rates allow for better evolutionary tracking of a dynamic environment, numerical calculations suggest that in our model the minimum average susceptible population, and hence the ESS, is achieved by a pathogen strain with zero mutation. We discuss how this result arises within our model and how the model might be modified to obtain a non-zero optimum.

**Keywords** mutation; eco-evolutionary dynamics; virulence; epidemic dynamics

## 1 Introduction

Evolutionary biologists have long been intrigued by the idea that mutation rates are themselves under evolutionary control. In particular, many have worked to answer questions such as how natural selection could lead to the evolution of lineages with non-zero mutation rates even though mutation generally lowers fitness in the short term (Fisher, 2000) and how mutation rates can be so consistent among very different genomes (Drake, 1991; Drake et al, 1998). Previous work has considered this problem for both sexual (e.g. Leigh, 1973; Johnson, 1999) and asexual populations (e.g. Kimura, 1960, 1967; Leigh, 1970; Orr, 2000). These classic studies focus on population-genetic models that include details such as recombination and modifier loci (see Sniegowski et al (2000) for a more detailed review of these works and Park and Krug (2013) for a more recent study). These works generally show that the population evolves to a non-zero mutation rate that balances the cost of generating phenotypes that vary around the optimum and the cost of failing to track the optimum in a changing environment due to lack of variation.

Department of Mathematics & Statistics,
McMaster University, Hamilton, Ontario L8S 4K1, Canada
E-mail: birchmd@mcmaster.ca

Here we instead take a quantitative genetic approach, not explicitly modelling alleles, modifier loci, etc. In particular, we examine the problem from an eco-evolutionary perspective, focusing on the evolution of pathogen virulence. This topic has been examined in recent experimental and theoretical work (Bolker et al, 2010; Berngruber et al, 2013; Herbeck et al, 2014) and is of general interest within the virology community (Holmes, 2013). We present a variation of the deterministic SIR compartmental model in epidemiology (Anderson and May, 1992) that includes a continuous distribution of virus strains differing in their virulence. Using diffusion of the distribution as a model of mutation, we investigate evolutionarily stable mutation rates in a periodically varying environment. In this model we include only the between host interactions of the pathogen, not the within-host dynamics (see Regoes et al (2013) for a study which considers within-host effects of viral agents).

## 2 Model

### 2.1 Full Model

For simplicity, we consider a phenomenological model of evolution. Rather than explicitly modelling the evolution of a modifier locus that increases mutation rate, we simply consider the invasibility or evolutionary stability of strains with different mutation rates, keeping track of the full spectrum of genotypes generated under mutation/selection balance with a given mutation rate. For further simplicity we treat our single trait (virulence; see below) as a quantitative-genetic rather than a Mendelian trait; consider only clonal replication; and neglect plasticity, assuming that there is a one-to-one map between genotype and phenotype.

Our model extends the one used by Bolker et al (2010) by adding a one-dimensional, continuous distribution of virulence and periodic variation in the base transmission rate. Let $S(t)$ and $I(t)$ be the density of susceptible and infectious individuals, respectively, in a population at time $t$. We treat virulence as a continuous property, in contrast to the discrete phenotypes used in population genetic studies, and consider a fixed one-to-one relationship between genotype and phenotype. Let $i(\alpha,t)$ be the density of infectious individuals at time $t$ which are infected with a strain of the pathogen with virulence $\alpha > 0$; thus the total infectious density is $I(t) = \int_0^\infty i(\alpha,t)\,d\alpha$. For simplicity, we assume a constant birth rate $\nu$. Let $\mu$ be the *per capita* natural (not disease-related) mortality rate. Let $\beta(\alpha,t)$ be the transmission rate for a pathogen strain with virulence $\alpha$ at time $t$, which is assumed to be a convex function of $\alpha$ (Alizon and Baalen, 2005), i.e. $\partial^2\beta/\partial\alpha^2 < 0$. The time dependence of $\beta$ allows for periodic forcing (with period $\tau$) in the transmission rate, which mimics seasonal variation in host contact patterns (social behaviour or effective density). The equations for this model are

$$\frac{dS}{dt} = \nu - S\int_0^\infty \beta(\alpha,t)i(\alpha,t)\,d\alpha - \mu S \tag{1a}$$

$$\frac{\partial i}{\partial t} = [S\beta(\alpha,t) - (\alpha+\mu)]i(\alpha,t) + D\frac{\partial^2 i}{\partial\alpha^2}, \tag{1b}$$

where the last term in (1b) models mutation of the virus (see Appendix A for details) at rate $D$. We use no-flux boundary conditions in (1b), i.e. $\partial i/\partial\alpha \to 0$ as $\alpha \to \infty$ and $(\partial i/\partial\alpha)|_{\alpha=0} = 0$, since mutation cannot change the total number of infectious individuals. Integrating (1b) over $\alpha$ we obtain

$$\frac{dI}{dt} = [S\langle\beta(\alpha,t)\rangle - (\langle\alpha\rangle+\mu)]I, \tag{2}$$

where $\langle\cdot\rangle$ denotes an average over the population of infectious individuals, i.e.

$$\langle f(\alpha,t)\rangle \equiv (1/I)\int_0^\infty f(\alpha,t)i(\alpha,t)\,d\alpha, \tag{3}$$

for any function $f(\alpha,t)$. Defining the virus population mean fitness as $d(\log I)/dt$, (2) motivates us to define the fitness, $w(\alpha,t)$, of each strain of the virus as

$$w(\alpha,t) \equiv S\beta(\alpha,t) - (\alpha+\mu), \tag{4}$$

so that $d(\log I)/dt = \langle w(\alpha,t)\rangle$. Since $\beta(\alpha,t)$ is convex, there is a strain of maximum fitness with virulence given by the solution to $S\cdot(\partial\beta/\partial\alpha)-1=0$ at each time $t$.

### 2.2 Moment Approximation

The partial differential equation (PDE) in this model makes it less analytically tractable than a coupled ordinary differential equation (ODE) model. Generalizing the simple technique used in Bolker et al (2010), we can approximate this model by a coupled ODE model using second order moment equations which track $S$, $I$, $\langle\alpha\rangle$, and the variance of virulence in the infectious population, $\sigma_\alpha^2$. Since the lower moments are coupled with higher ones, a *moment closure* technique is needed (Lloyd, 2004). Here we assume that the distribution of $i$ is Gaussian so that the higher order cumulants are zero; this is a typical assumption in genetic models (but cf. Turelli and Barton (1994)). In deriving the moment equations $\beta(\alpha,t)$ is expanded as a Taylor series in $\alpha$, which is also truncated to second order; we assume that the dynamics occur far from the boundary so that $i(0,t)\approx 0$ for all $t$. The full derivation of the moment equations is given in Appendix B. The resulting moment equations are

$$\frac{dS}{dt} = \nu - SI\left[\beta(\langle\alpha\rangle,t) + \frac{1}{2}\sigma_\alpha^2\beta_{\alpha\alpha}(\langle\alpha\rangle,t)\right] - \mu S \tag{5a}$$

$$\frac{dI}{dt} = \left[S\beta(\langle\alpha\rangle,t) - (\langle\alpha\rangle+\mu)\right]I + \frac{1}{2}SI\sigma_\alpha^2\beta_{\alpha\alpha}(\langle\alpha\rangle,t) \tag{5b}$$

$$\frac{d\langle\alpha\rangle}{dt} = \sigma_\alpha^2\left[S\beta_\alpha(\langle\alpha\rangle,t) - 1\right] \tag{5c}$$

$$\frac{d\sigma_\alpha^2}{dt} = \left[\sigma_\alpha^2\right]^2 S\beta_{\alpha\alpha}(\langle\alpha\rangle,t) + 2D, \tag{5d}$$

where subscript $\alpha$'s on $\beta$ denote derivatives in $\alpha$, e.g. $\beta_{\alpha\alpha}\equiv\partial^2\beta/\partial\alpha^2$ (the time-dependence of the state variables $\{S,I,\langle\alpha\rangle,\sigma_\alpha^2\}$ is suppressed for brevity).

## 3 Numerical Methods

In order to obtain numerical solutions to (1) we use a uniformly spaced discretization of the $\alpha$ axis, $\{\alpha_j\}_{j=1}^N$, where $\alpha_1=0$ and $\alpha_N$ is chosen to be large enough such that $i(\alpha_N,t)\approx 0$ for all times. Thus, given $\{i_j(t)\equiv i(\alpha_j,t)\}_{j=1}^N$ at a fixed time $t$, we can compute the integral in (1a) using the trapezoidal rule and the second derivative in (1b) using a centred-difference finite differencing scheme. We approximate the

PDE in the time axis as a sequence of first order coupled ODEs for the functions $\{i_j(t)\}$ defined previously. Then (1) becomes

$$\frac{dS}{dt} = \nu - S\frac{\Delta\alpha}{2}\sum_{j=1}^{N-1}[\beta(\alpha_{j+1},t)i_{j+1} - \beta(\alpha_j,t)i_j] - \mu S \tag{6a}$$

$$\frac{di_j}{dt} = [S\beta(\alpha_j,t) - (\alpha_j+\mu)]i_j + D\frac{i_{j+1}-2i_j+i_{j-1}}{\Delta\alpha^2},\ 2 \le j \le N-1, \tag{6b}$$

where $\Delta\alpha = \alpha_{j+1} - \alpha_j$ is the spacing of the discretization in $\alpha$. Appropriate adjustments must be made for the boundary equations $i_1$ and $i_N$ to implement the boundary conditions. In particular,

$$\frac{di_1}{dt} = [S\beta(\alpha_1,t) - (\alpha_1+\mu)]i_1 + D\frac{i_2-i_1}{\Delta\alpha^2}, \tag{7}$$

to enforce $\partial i/\partial\alpha = 0$ at $\alpha = 0$ and

$$\frac{di_N}{dt} = [S\beta(\alpha_N,t) - (\alpha_N+\mu)]i_N + D\frac{-2i_N+i_{N-1}}{\Delta\alpha^2}, \tag{8}$$

to enforce $i(\alpha,t) = 0$ for $\alpha > \alpha_N$. This system of coupled ODEs is then solved using the R programming language (version 3.1.0) using the `lsoda` integrator from the `deSolve` package (version 1.10) (R Core Team, 2014; Soetaert et al, 2010).

For numerical solutions, we must specify a particular functional form for $\beta(\alpha,t)$; following Bolker et al (2010) we chose a power law trade-off curve. We also add sinusoidal seasonal forcing in this work, so $\beta(\alpha,t)$ has the form

$$\beta(\alpha,t) = c\alpha^{1/\gamma}\left[1+\delta\sin\left(\frac{2\pi t}{\tau}\right)\right], \tag{9}$$

where $c > 0$, $\gamma > 1$ and $0 \le \delta < 1$. We call $\delta$ the seasonal forcing amplitude and $\tau$ the seasonal period. We can reduce the space of parameters in the model by nondimensionalizing, working in units where $\nu = \mu = 1$. There are thus five parameters of interest: $c$, $\delta$, $\gamma$, $\tau$ and $D$.

## 4 Results

### 4.1 Maximum viable mutation rate

First assume a constant environment so that $\beta(\alpha,t) = \beta_0(\alpha)$ (i.e. $\delta = 0$). As the pathogen initially invades we assume that $I(t) \ll S_{*,\mathrm{df}}$, where $S_{*,\mathrm{df}} = \nu/\mu$ is the disease free equilibrium. Since $\beta_0$ is time-independent we can separate variables in (1b), writing $i(\alpha,t) = I(t)\lambda(\alpha)$, where $\int_0^\infty \lambda(\alpha)\,d\alpha = 1$, to obtain

$$\dot{I} + (C+\mu)I = 0 \tag{10}$$

$$D\lambda'' + (\beta_0(\alpha)S - \alpha + C)\lambda = 0, \tag{11}$$

where $C$ is a constant of separation, a dot ($\dot{}$) is used to denote a time derivative and a prime ($'$) is used to denote a derivative in $\alpha$. The solution to (10) is $I \propto \exp(-(C+\mu)t)$, therefore, the pathogen cannot invade the population if $C+\mu > 0$. Let $\alpha_0$ be the virulence of the strain with maximum fitness (i.e. $S\beta_0'(\alpha_0) - 1 = 0$). Then expanding $\beta_0$ to second order about $\alpha_0$, (11) becomes

$$D\lambda'' + \left(S\beta_0(\alpha_0) - \alpha_0 + C + \frac{1}{2}S\beta_0''(\alpha_0)(\alpha-\alpha_0)^2\right)\lambda = 0. \tag{12}$$

The Gaussian probability density, $y \propto \exp\left(-(x-m)^2/(2\sigma^2)\right)$, is a solution to the differential equation

$$\frac{d^2y}{dx^2} + \left(\frac{1}{\sigma^2} - \frac{1}{\sigma^4}(x-m)^2\right) y = 0. \tag{13}$$

Comparing this fact with (12), it must be the case that

$$\frac{S\beta_0(\alpha_0) - \alpha_0 + C}{D} = \sqrt{-\frac{S\beta_0''(\alpha_0)}{2D}} \tag{14}$$

for there to be a normalizable solution[1]. Note that the negative sign under the square root in (14) is not a problem because we have assumed $\beta_0$ is convex. We can rewrite this condition in terms of the fitness, defined in (4), as

$$-2\frac{[w(\alpha_0) + (C+\mu)]^2}{w''(\alpha_0)} = D \tag{15}$$

From (15) and the condition that $C+\mu > 0$, we conclude that invasion of the pathogen in the population is impossible if

$$D > -2\frac{[w(\alpha_0)]^2}{w''(\alpha_0)} \equiv D_{\max}. \tag{16}$$

Therefore, $D_{\max}$ represents a maximum viable mutation rate for the pathogen. We again note that the convexity of $\beta_0(\alpha)$ makes $w''(\alpha_0) < 0$ so that $D_{\max} > 0$.

We can now ask if this maximum mutation rate changes when seasonal forcing is included in the model. We might guess that a higher mutation rate would be advantageous due to the ability of a pathogen with a high mutation rate to adapt to the changing environment. Let $\beta(\alpha,t) = (1+\delta g(t))\beta_0(\alpha)$, where $g(t)$ has mean zero, period $\tau$ and $|g(t)| \leq 1$ for all $t$. The parameter $\delta$ gives the strength of the seasonal forcing. Assume first that $\delta$ is small so that this case can be considered a perturbation of the unforced model. We can then construct a solution in powers of $\delta$,

$$S(t) = S^{(0)}(t) + \delta S^{(1)}(t) + \delta^2 S^{(2)}(t) + \cdots \tag{17}$$

$$i(\alpha,t) = i^{(0)}(\alpha,t) + \delta i^{(1)}(\alpha,t) + \delta^2 i^{(2)}(\alpha,t) + \cdots. \tag{18}$$

The zeroth order equations will be the unforced equations analysed previously, hence we have the mutation rate limit as in (16). If we assume $D > D_{\max}$, then $i^{(0)} \to 0$. Then the first order equation becomes

$$\frac{\partial i^{(1)}}{\partial t} = \left[S^{(0)}\beta_0(\alpha) - (\alpha+\mu)\right] i^{(1)}(\alpha,t) + D\frac{\partial^2 i^{(1)}}{\partial \alpha^2}, \tag{19}$$

which is of the same form as the unforced model. Hence, $i^{(1)}$ will also tend to zero by the same argument as for the unforced model. Similarly, one can show by induction that when $i^{(j)} \to 0$ for $j < k$ then the $k$-th order equation is of the same form as the unforced model and therefore $i^{(k)} \to 0$. Since corrections of all orders tend to zero in the perturbation, the size of $\delta$ is unimportant (so long as $\delta < 1$, which is required regardless to ensure that $\beta(\alpha,t) \geq 0$ for all $t$) and so the same limit as in (16) holds in the seasonally forced case as well.

[1] (13) is a second order, linear ODE so there are two linearly independent solutions, however only one of them (the Gaussian probability density) is normalizable so that the integral of the solution is equal to unity.

### 4.2 Evolutionarily Stable Mutation Rate

We established in the previous section that there is a maximum mutation rate, $D_{\max}$, beyond which the pathogen cannot emerge into a population. We can now answer the question as to whether there is an evolutionarily stable mutation rate, $D_{\text{ess}}$, such that $0 \leq D_{\text{ess}} < D_{\max}$. Here we define evolutionarily stable to mean that the population of pathogens with mutation rate $D_{\text{ess}}$ cannot be invaded by a population of pathogens with a different mutation rate. To answer this question we consider a two-strain version of the model, where the strains differ only in their mutation rates. This model is described by the equations

$$\frac{dS}{dt} = \nu - S(t)\int_0^\infty \beta(\alpha,t)\left[i_1(\alpha,t)+i_2(\alpha,t)\right]\,d\alpha - \mu S(t) \tag{20a}$$

$$\frac{\partial i_1}{\partial t} = [S(t)\beta(\alpha,t)-(\alpha+\mu)]i_1(\alpha,t) + D_1\frac{\partial^2 i_1}{\partial \alpha^2} \tag{20b}$$

$$\frac{\partial i_2}{\partial t} = [S(t)\beta(\alpha,t)-(\alpha+\mu)]i_2(\alpha,t) + D_2\frac{\partial^2 i_2}{\partial \alpha^2}. \tag{20c}$$

We shall investigate strain 2 invading strain 1 by perturbing the steady-state of this system where $S(t) = S_{1,*}(t)$, $i_1(\alpha,t) = i_{1,*}(\alpha,t)$, $i_2(\alpha,t) = 0$. Here, $S_{1,*}$ and $i_{1,*}$ denote the steady-states of the monoculture (single pathogen model). Writing $i_2(\alpha,t) = 0 + \varepsilon i_2^{(1)}(\alpha,t)$, thinking of $\varepsilon$ as a small perturbation parameter, the first order expression for the dynamics of $I_2^{(1)}(t) = \int_0^\infty i_2^{(1)}(\alpha,t)\,d\alpha$ is

$$\frac{dI_2^{(1)}}{dt} = \left[S_{1,*}\left\langle\beta(\alpha,t)\right\rangle_2 - \left(\left\langle\alpha\right\rangle_2+\mu\right)\right]I_2^{(1)}, \tag{21}$$

where $\langle\cdot\rangle_2$ denotes an average over the population of strain 2 infectious individuals. Rearranging (21) and taking time averages we have

$$\overline{\frac{d}{dt}\left(\log I_2^{(1)}\right)} = \overline{S_{1,*}(t)}\;\overline{\left\langle\beta(\alpha,t)\right\rangle_2} - \left(\overline{\left\langle\alpha\right\rangle_2}+\mu\right) + \operatorname{cov}(S_{1,*},\left\langle\beta(\alpha,t)\right\rangle_2), \tag{22}$$

where a bar denotes a time average. Since the time dependence of $\beta$ is the seasonal forcing, $\operatorname{cov}(S_{1,*},\langle\beta(\alpha,t)\rangle_2) < 0$ due to $\langle\beta(\alpha,t)\rangle_1$ increasing whenever $\langle\beta(\alpha,t)\rangle_2$ is increasing and an increase in $\langle\beta(\alpha,t)\rangle_1$ results in a decrease of $S_{1,*}$. Therefore, invasion by strain 2 will be impossible if $\overline{S_{1,*}(t)}\;\overline{\langle\beta(\alpha,t)\rangle_2} - \left(\overline{\langle\alpha\rangle_2}+\mu\right) < 0$. We can make analytical progress with this criterion by assuming that the time averaged values in (22) are close to the equilibrium values of their respective unforced monocultures (by unforced we mean $\beta(\alpha,t)$ becomes $\beta_0(\alpha)$, where $\overline{\beta(\alpha,t)} = \beta_0(\alpha)$). From (2) it is clear that $S_* = (\langle\alpha\rangle_* + \mu)/\langle\beta_0(\alpha)\rangle_*$, where subscript asterisks denote equilibrium in the unforced, single pathogen model. We then have

$$\left(\left\langle\alpha\right\rangle_{1,*}+\mu\right)\frac{\left\langle\beta_0(\alpha)\right\rangle_{2,*}}{\left\langle\beta_0(\alpha)\right\rangle_{1,*}} - \left(\left\langle\alpha\right\rangle_{2,*}+\mu\right) < 0. \tag{23}$$

We can simplify the criterion further if we assume that the equilibrium values of the full model monocultures are close to the equilibrium of the moment equations. We see from (5c) that $S_* = 1/\beta_0'(\langle\alpha\rangle_*)$, and after some simplification the criterion becomes

$$\left(\left\langle\alpha\right\rangle_{2,*}+\mu\right)\left(\frac{S_{1,*}}{S_{2,*}}-1\right) < 0. \tag{24}$$

Therefore, strain 2 cannot invade strain 1 if

$$S_{2,*} > S_{1,*} \tag{25}$$

because the average growth rate of the invader would be negative. This criterion was derived using a few simplifying assumptions, but motivated by the result, we conjecture that invasion is impossible if $\overline{S_{2,*}(t)} > \overline{S_{1,*}(t)}$, where the notation here is for the time average of the steady state of the respective seasonally forced monocultures.

### 4.3 Numerical Results

The necessary invasion criterion $\overline{S_{2,*}(t)} \leq \overline{S_{1,*}(t)}$ derived in the previous section relies critically on the assumption that the time averaged parameters in the steady state of the forced model are approximately equal to the equilibrium values in the corresponding unforced model, i.e. $\overline{S_*(t)} \approx S_{*,\text{unforced}}$. For notational simplicity, we will denote the equilibrium number of susceptible individuals in the unforced model by $S_{\text{uf}*}$ for the remainder of this section.

We investigate how well this assumption holds, and its effect on invasion dynamics, by comparing the numerical solutions of the full model to those of the unforced model. $\overline{S_*(t)}$ is determined by solving (1) numerically as described in section 3 until steady state is reached and taking the mean of $S_*(t)$ over at least two periods. The period of $S_*(t)$ was taken to be equal to $\tau$ since over the range of parameters used for the calculations this was always observed to be the case (there was no evidence of period doubling or other routes to chaos). $S_{\text{uf}*}$ can be computed without solving the full PDE model since the equilibrium is not time dependent in the unforced model and so we can separate variables as in subsection 4.1 in order to obtain the following ODE:

$$D\lambda''(\alpha) + (\beta_0(\alpha)S_{\text{uf}*} - (\alpha+\mu))\,\lambda(\alpha) = 0, \tag{26}$$

where $i_{\text{uf}*}(\alpha,t) = I_{\text{uf}*}\lambda(\alpha)$ is the equilibrium density of infectious individuals and $\int_0^\infty \lambda(\alpha)\,d\alpha = 1$. The boundary condition at the origin on the PDE also carries over to $\lambda$: $\lambda'(0) = 0$. This ODE with boundary conditions is a Sturm-Liouville problem (much like the one-dimensional time-independent Schrödinger equation) where $S_{\text{uf}*}$ is the eigenvalue. Thus, it can be solved by systematically varying $S_{\text{uf}*}$ and integrating (26) with initial conditions satisfying the boundary condition at zero until a normalizable solution is found. We furthermore assumed that the equilibrium of the full model was close to that of moment equation approximation. One can show that the equilibrium density of susceptible individuals in (5) is

$$S_{\text{uf}*} = \frac{1}{\beta'(\langle\alpha\rangle_*)}, \tag{27}$$

where $\langle\alpha\rangle_*$ satisfies

$$\langle\alpha\rangle_* + \mu = \frac{\beta(\langle\alpha\rangle_*)}{\beta'(\langle\alpha\rangle_*)} - \sqrt{-\frac{D\beta''(\langle\alpha\rangle_*)}{\beta'(\langle\alpha\rangle_*)}}. \tag{28}$$

Eq. 28 must be solved numerically for $\langle\alpha\rangle_*$. The results comparing the three equilibrium calculations to the corresponding forced model are shown in Figure 1. The results indicate that the approximation $\overline{S_*(t)} \approx S_{\text{uf}*}$ is valid to within $\sim 15\%$ for the

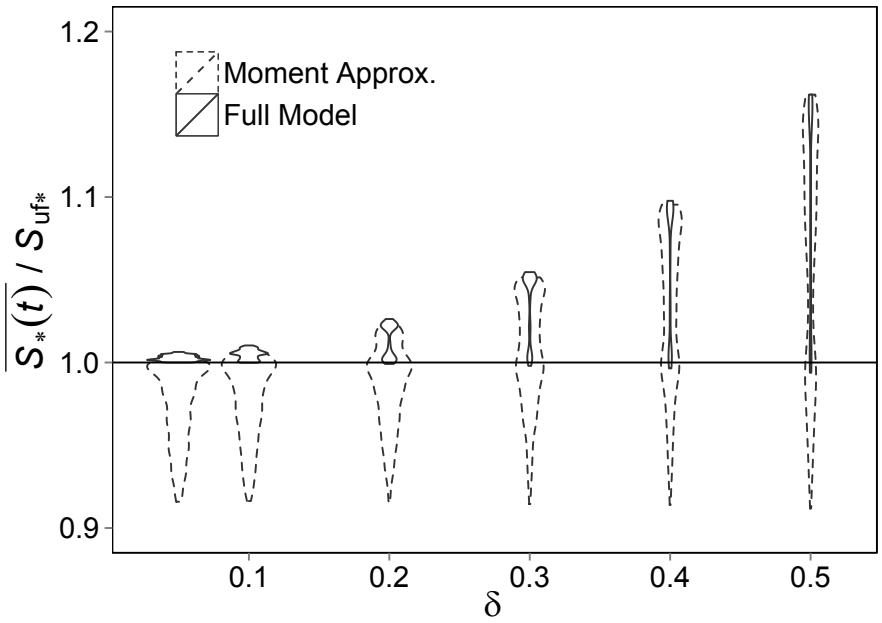


Fig. 1: Violin plot of the ratio of the equilibrium density of susceptible individuals in the forced model ($\overline{S_*(t)}$) to the equilibrium density in the corresponding unforced model ($S_{\mathrm{uf}*}$) as a function of $\delta$ for both an exact calculation of the full PDE model (solid; (26)) and the moment approximation (dashed; (27)). These data represent the results of 13558 different calculations with parameters chosen in an ad-hoc manner from the ranges $\gamma = 1.5 - 2.75$, $c = 3 - 13$, $\tau = 0.5 - 20$, and $D = 0.02 - 0.71$. The unforced calculations are accurate to within 15% or better for all parameter values.

parameter values tested and appears to grow quadratically with $\delta$. Thus, while the approximation is not perfect, the equilibrium estimates of the unforced moment equation approximation are not so far off as to change the qualitative conclusion of the necessary invasion criterion.

Finally, given that the evolutionarily stable strain has the lowest value of $\overline{S_*(t)}$, we can consider $\overline{S_*(t)}$ as a function of $D$ for a variety of parameter values (i.e. values of $c$, $\delta$, $\gamma$, $\tau$). Figure Figure 2 shows that $\overline{S_*(t)}$ is an increasing function of $D$ for all parameter values, suggesting that $D = 0$ is indeed the evolutionarily stable mutation rate across a wide range of parameter space.

## 5 Discussion

The conclusion from the previous section is that the evolutionarily stable pathogen is the one which has the smallest *average* number of susceptible individuals in the population once steady state has been reached. This is a reasonable criterion since the average steady state $S$ measures well a strain can draw down the constant influx of new susceptible individuals ($\nu$), and accords well with a variety of classic results in ecology and epidemiology that link ability to deplete resources with competitive dominance (Tilman, 1982). One novel aspect of our results is that the criterion holds

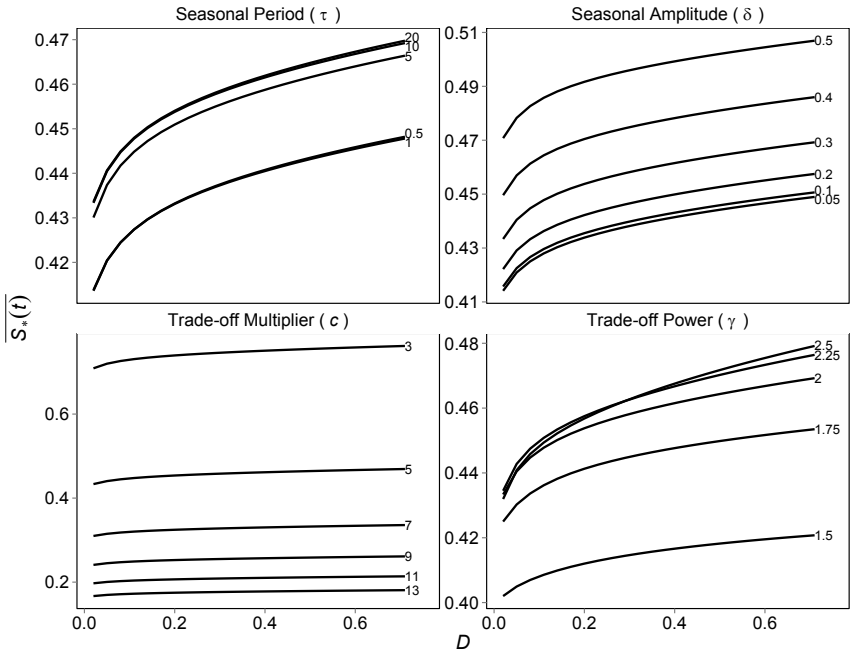


Fig. 2: Plots of the equilibrium density of susceptibles in the forced model ($\overline{S_*(t)}$) as a function of $D$. Each plot allows one additional parameter to vary. The base set of parameters is $\gamma = 2$, $c = 5$, $\delta = 0.3$ and $\tau = 10$. the bottom right plot varies $\gamma$ from 1.5 to 2.5; the bottom left plot varies $c$ from 3 to 13; the top right plot varies $\delta$ from 0.05 to 0.5; the top left plot varies $\tau$ from 1 to 20. The label next to each line indicates the value of the parameter which is varying.

even in a periodically varying environment, which in other contexts can allow for invasion, and coexistence, by strains other than the one with the greatest ability to deplete the resource (e.g. Cushing, 1980).

This criterion together with the numerical results (see Figure 2) suggests that $D_{\text{ess}} = 0$. This result seems to contradict previous theoretical population genetic studies that have found optimal mutation rates greater than zero. To understand our result we first note that by expanding the population mean fitness, $\langle w(\alpha,t)\rangle$, about the optimum virulence, $\alpha_0(t)$, to second order we can partition the fitness into three terms

$$\langle w(\alpha,t)\rangle = w_0(t) - w_{\text{mut}}(t) - w_{\text{track}}(t), \tag{29}$$

where $w_0(t)$ is the maximum fitness at time $t$, while

$$w_{\text{mut}}(t) = -\frac{1}{2} S\beta_{\alpha\alpha}(\alpha_0,t)\sigma_\alpha^2 \tag{30}$$

and

$$w_{\text{track}}(t) = -\frac{1}{2} S\beta_{\alpha\alpha}(\alpha_0,t)\left(\langle\alpha\rangle - \alpha_0\right)^2 \tag{31}$$

give the loss of fitness due to mutation load (30) and imperfect tracking of the optimum by the population mean (31), respectively. Given this partition, the qualitative reasoning for the existence of a non-zero optimum mutation rate is that we

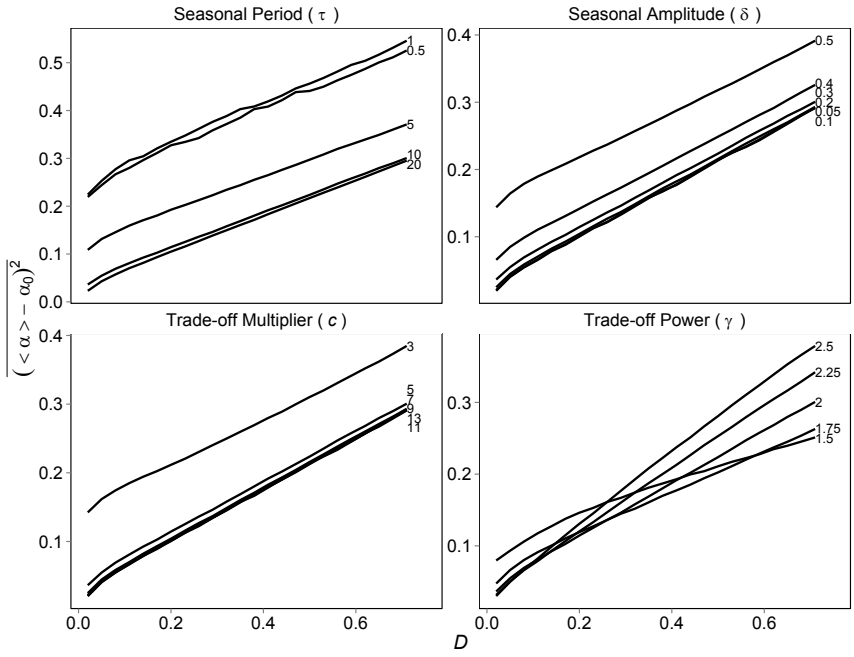


Fig. 3: Plots of the (temporal) mean square difference between the population average and optimal virulences, $(\langle\alpha\rangle - \alpha_0)^2$, as a function of $D$. Each plot allows one additional parameter to vary. The base set of parameters is $\gamma = 2$, $c = 5$, $\delta = 0.3$ and $\tau = 10$. the bottom right plot varies $\gamma$ from 1.5 to 2.5; the bottom left plot varies $c$ from 3 to 13; the top right plot varies $\delta$ from 0.05 to 0.5; the top left plot varies $\tau$ from 1 to 20. The label next to each line indicates the value of the parameter which is varying.

expect $w_{\text{mut}}$ to increase as a function of mutation rate $D$ while $w_{\text{track}}$ decreases, with the minimum total load at some intermediate value. However, in this system, $(\langle\alpha\rangle - \alpha_0)^2$ is correlated with $\sigma_\alpha^2$ so that $w_{\text{track}}$ in fact increases as a function of $D$ (Figure 3). Thus, increasing mutation rate *decreases* the population's ability to track the time-varying optimum genotype!

The squared deviation of the mean genotype from the optimum ($(\langle\alpha\rangle - \alpha_0)^2$) and the genotypic variance ($\sigma_\alpha^2$) are correlated because of the boundary at $\alpha = 0$. Due to the zero-derivative boundary condition (which was required to enforce conservation of infectious density by the diffusion), when $\sigma_\alpha$ is comparable to (or greater than) $\langle\alpha\rangle$, the distribution cannot be symmetric because of "reflection" of infectious density at $\alpha = 0$. If, in addition, $\alpha_0$ is also comparable to (or less than) $\sigma_\alpha$ then $\langle\alpha\rangle$ will not be able to effectively track $\alpha_0$ due to the asymmetry of the distribution forcing the population average to higher values. To see this effect, we compare a typical situation of $\gamma = 1.5$ to $\gamma = 2$. Notice that the slopes of the lines in the bottom right panel of Figure 3 indicate that the effect should be stronger in the latter case. Figure 4a shows $\langle\alpha\rangle$ and $\alpha_0$ as a function of $t$ after steady state has been reached for $\gamma = 1.5$, while Figure 4b shows the same plot for $\gamma = 2$. In both cases $\overline{\sigma_\alpha}$ is shown for reference. In both cases there is a systematic shift of the temporal

mean value of $\langle\alpha\rangle$ above that of $\alpha_0$; the shift is larger in the $\gamma = 2$ case because $\sigma_\alpha$ is closer to $\alpha_0$.

As one final visualization of this effect, we show $i(\alpha,t)$ at $t = 127.45$ in the two cases considered in the example above. These distributions are plotted in Figure 5. Notice that $\alpha_0$ is close to the peak of the distribution in both cases, however due to the greater asymmetry of the distribution in the $\gamma = 2$ case, the mean is displaced farther from the peak.

Once again considering Figure 2, notice that $\overline{(\langle\alpha\rangle - \alpha_0)^2}$ scales linearly with $D$. A similar set of plots (not shown) indicates that $\sigma_\alpha^2$ scales with $\sqrt{D}$. Since these factors correspond to $w_{\text{track}}$ and $w_{\text{mut}}$, such a scaling law would suggest that an intermediate optimum *would* exist if $w_{\text{track}}$ decreased with increased mutation rate, since in that case, as we expected initially, the two fitness components should cross.

Thus, our primary result that evo-epidemiological dynamics should drive the pathogen toward a minimal mutation rate depends strongly on the assumption of a barrier in trait space at zero virulence. While there is some evidence that bacterial parasites (for example) cannot easily switch from parasitism to mutualism (Moran and Wernegreen, 2000, i.e. negative virulence), it is not clear whether our no-flux boundary represents a realistic model of this constraint. Similarly, we suspect that removing the boundary by modeling virulence on a logarithmic scale might change the qualitative dynamics; this change would also raise the question of whether changes in virulence are more appropriately modeled by an arithmetic or geometric random walk. Finally, we note that although several of our results, such as the relative advantage of strains that most reduce the period-averaged density of susceptibles, are independent of the quantitative details of the model, the numerical simulations we use to confirm the approximate results may be sensitive. In particular, several previous studies of evolutionary and evo-epidemiological dynamics of virulence have pointed to the sensitivity of such dynamics to the detailed shape of the tradeoff curve (Alizon and Baalen, 2005; Bolker et al, 2010), and to our lack of knowledge about these shapes (Froissart et al, 2010).

## 6 Conclusion

In this work we have used a deterministic, compartmental epidemiological model with seasonal forcing to study the evolution of virulence in a pathogen. We used this situation to consider the problem of evolutionarily stable mutation rates in an eco-evolutionary context. Within this model we derived a maximum mutation rate, $D_{\text{max}}$, beyond which the pathogen will fail to invade a wholly susceptible population. We also derived a criterion for the evolutionarily stable mutation rate, $D_{\text{ess}}$, which suggested that the pathogen with the minimum average number of susceptible individuals in the population, once the steady-state has been reached, should be the one with the evolutionarily stable mutation rate. Numerical calculations provided evidence that $D_{\text{ess}} = 0$, however this appears to be a result of the boundary at $\alpha = 0$. Future work may wish to consider variants of the present model where the virulence domain is the whole real line, as $D_{\text{ess}} > 0$ may be possible in a situation without a boundary.

**Acknowledgements** The authors thank the Natural Sciences and Engineering Research Council of Canada (NSERC) for their financial support of this work.

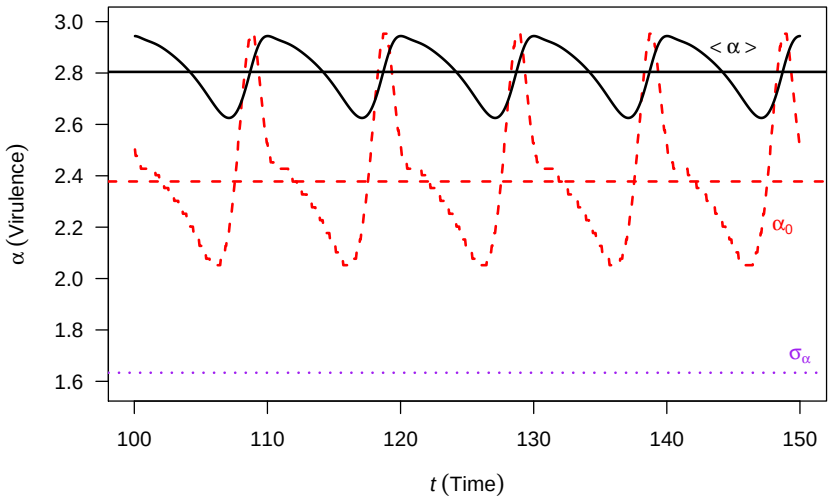


(a)

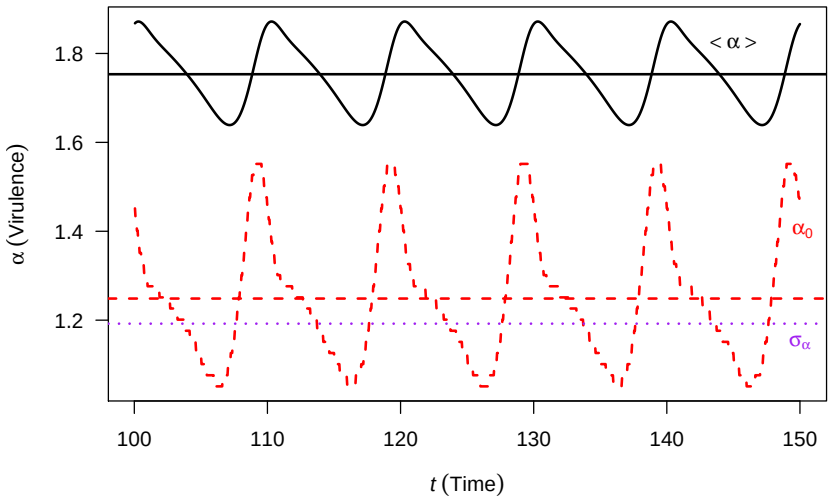


(b)

Fig. 4: Typical plots of the population mean virulence, $\langle\alpha\rangle$ (black; solid), and optimum virulence, $\alpha_0$ (red; dashed), as a function of $t$ after a steady state has been reached. The horizontal lines of the same type show the temporal mean values. (a) shows a case where $\gamma = 1.5$, while (b) shows a case where $\gamma = 2$ (all other parameters are idenitcal in the two cases). The dotted puple line shows the temporal mean value of $\sigma_\alpha$. When $\sigma_\alpha \simeq \alpha_0$, $\langle\alpha\rangle$ is biased towards higher values, preventing proper tracking of the optimal value.

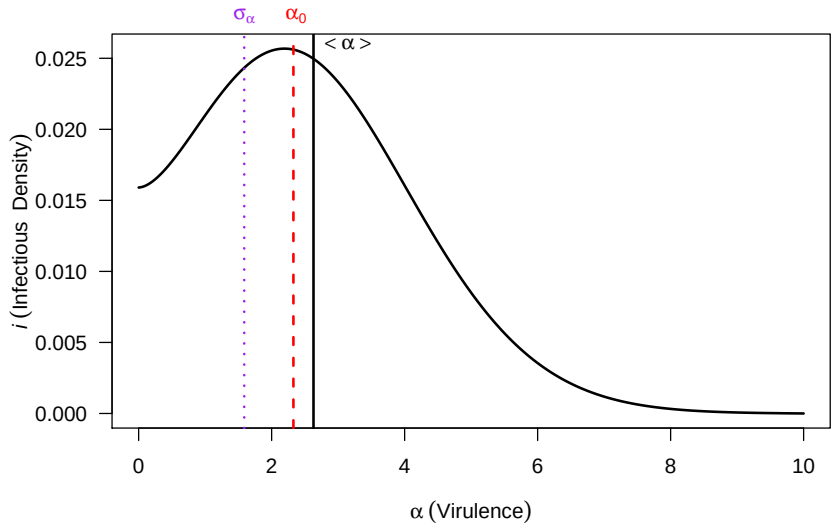


(a)

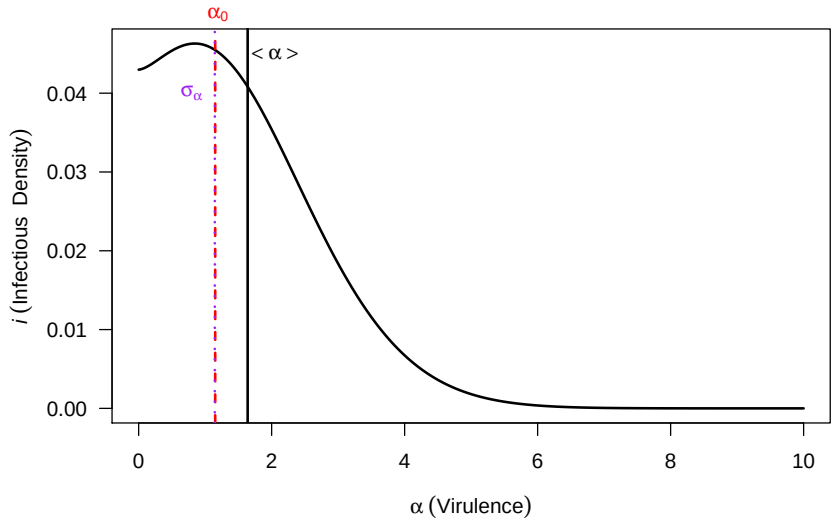


(b)

Fig. 5: Plots of $i(\alpha,t)$ at $t = 127.45$ for the same parameter values as Figure 4 ((a) again corresponds to $\gamma = 1.5$ and (b) again corresponds to $\gamma = 2$). The solid vertical line shows the population mean value of the distribution, the red dashed vertical line shows the optimal virulence, $\alpha_0$, at that time and the purple dotted line shows the standard deviation of the distribution, $\sigma_\alpha$. The boundary at $\alpha = 0$ causes an asymmetry in the distribution which biases the population mean virulence to higher values, away from the optimum.

## References


Alizon S, Baalen M (2005) Emergence of a convex trade-off between transmission and virulence. The American Naturalist 165(6):E155–E167

Anderson RM, May RM (1992) Infectious Diseases of Humans: Dynamics and Control. Oxford University Press

Berngruber TW, Froissart R, Choisy M, Gandon S (2013) Evolution of virulence in emerging epidemics. PLoS Pathog 9(3):e1003,209

Bolker BM, Nanda A, Shah D (2010) Transient virulence of emerging pathogens. J R Soc Interface 7(46):811–822

Cushing JM (1980) Two species competition in a periodic environment. Journal of Mathematical Biology 10(4):385–400, DOI 10.1007/BF00276097, URL http://link.springer.com/article/10.1007/BF00276097

Drake JW (1991) A constant rate of spontaneous mutation in DNA-based microbes. PNAS 88(16):7160–7164

Drake JW, Charlesworth B, Charlesworth D, Crow JF (1998) Rates of spontaneous mutation. Genetics 148(4):1667–1686

Fisher RA (2000) The Genetical Theory of Natural Selection. Oxford University Press, Oxford, (ed. H. Bennett)

Froissart R, Doumayrou J, Vuillaume F, Alizon S, Michalakis Y (2010) The virulencetransmission trade-off in vector-borne plant viruses: a review of (non-)existing studies. Philosophical Transactions of the Royal Society B: Biological Sciences 365(1548):1907–1918, DOI 10.1098/rstb.2010.0068, URL http://rstb.royalsocietypublishing.org/content/365/1548/1907

Herbeck JT, Mittler JE, Gottlieb GS, Mullins JI (2014) An HIV epidemic model based on viral load dynamics: Value in assessing empirical trends in HIV virulence and community viral load. PLoS Comput Biol 10(6):e1003,673

Holmes EC (2013) What can we predict about viral evolution and emergence? Current Opinion in Virology 3(2):180–184

Johnson T (1999) Beneficial mutations, hitchhiking and the evolution of mutation rates in sexual populations. Genetics 151(4):1621–1631

Kimura M (1960) Optimum mutation rate and degree of dominance as determined by the principle of minimum genetic load. J Genet 57(1):21–34

Kimura M (1967) On the evolutionary adjustment of spontaneous mutation rates. Genetics Research 9(01):23–34

Leigh EG (1973) The evolution of mutation rates. Genetics 73:Suppl 73:1–18

Leigh EG Jr (1970) Natural selection and mutability. The American Naturalist 104(937):301–305

Lloyd AL (2004) Estimating variability in models for recurrent epidemics: assessing the use of moment closure techniques. Theoretical Population Biology 65(1):49–65

Moran NA, Wernegreen JJ (2000) Lifestyle evolution in symbiotic bacteria: insights from genomics. Trends in Ecology & Evolution 15(8):321–326, DOI 10.1016/S0169-5347(00)01902-9, URL http://www.sciencedirect.com/science/article/pii/S0169534700019029

Orr HA (2000) The rate of adaptation in asexuals. Genetics 155(2):961–968

Park SC, Krug J (2013) Rate of adaptation in sexuals and asexuals: A solvable model of the Fisher-Muller effect. Genetics 195(3):941–955

R Core Team (2014) R: A Language and Environment for Statistical Computing. R Foundation for Statistical Computing, Vienna, Austria, URL http://www.R-project.org/

Regoes RR, Hamblin S, Tanaka MM (2013) Viral mutation rates: modelling the roles of within-host viral dynamics and the trade-off between replication fidelity and speed. Proceedings of the Royal Society of London B: Biological Sciences 280(1750):20122,047

Sniegowski PD, Gerrish PJ, Johnson T, Shaver A (2000) The evolution of mutation rates: separating causes from consequences. Bioessays 22(12):1057–1066

Soetaert K, Petzoldt T, Setzer RW (2010) Solving differential equations in R: Package deSolve. Journal of Statistical Software 33(9):1–25, URL http://www.jstatsoft.org/v33/i09

Tilman D (1982) Resource competition and community structure. Princeton University Press, Princeton, NJ

Turelli M, Barton NH (1994) Genetic and statistical analyses of strong selection on polygenic traits: What, me normal? Genetics 138(3):913 –941, URL http://www.genetics.org/content/138/3/913.abstract

## A General mutation spectrum

Generally, one could write (1b) as

$$\frac{\partial i}{\partial t} = [S(t)\beta(\alpha,t) - (\alpha+\mu)]i(\alpha,t) - mi(\alpha,t) + m\int_0^\infty K(\alpha',\alpha)i(\alpha',t)\,d\alpha', \tag{32}$$

where $m$ is the mutation rate (although a different mutation rate than $D$ defined below) and $K(\alpha',\alpha)$ is the mutation spectrum (the rate of mutation from strain $\alpha'$ to $\alpha$). $K(\alpha',\alpha)$ must have the following properties:

(i) $K(\alpha',\alpha) \geq 0$ for all $\alpha',\alpha \in [0,\infty)$
(ii) $\int_0^\infty K(\alpha',\alpha)\,d\alpha = 1$.

Property (i) follows from probabilities of mutation being non-negative and property (ii) ensures that mutation cannot change the total number of infectious individuals. This mutation spectrum can accommodate very general models of mutation (even among discrete phenotypes through the use of Dirac delta functions). Our diffusion model of mutation follows from this general spectrum under the assumptions that $K(\alpha',\alpha)$ is symmetric in the sense that

$$K(\alpha',\alpha) = K(\alpha,\alpha') \tag{33}$$

and for each $\alpha$, $K(\alpha',\alpha)$ is narrowly peaked such that

$$\int_0^\infty K(\alpha',\alpha)i(\alpha',t)\,d\alpha' \approx \int_0^\infty K(\alpha',\alpha)\left[i(\alpha,t) + \frac{\partial i}{\partial \alpha}(\alpha'-\alpha) + \frac{1}{2}\frac{\partial^2 i}{\partial \alpha^2}(\alpha'-\alpha)^2\right]d\alpha'. \tag{34}$$

Using (33) and (34), as well as applying property (ii), in (32) we obtain

$$\frac{\partial i}{\partial t} = [S(t)\beta(\alpha,t) - (\alpha+\mu)]i(\alpha,t) + D(\alpha)\frac{\partial^2 i}{\partial \alpha^2}, \tag{35}$$

where $D(\alpha) \equiv (m/2)\int_0^\infty (\alpha'-\alpha)^2 K(\alpha',\alpha)\,d\alpha'$. Finally, we obtain (1b) by assuming that $D(\alpha)$ is constant for all $\alpha$.

## B Derivation of Second Order Moment Equations

Here we wish to approximate the full model, given by (1), by characterising the infectious distribution, $i(\alpha,t)$, according to its first two moments. In addition, we shall assume that $i(\alpha,t)$ is normally distributed in $\alpha$ for every $t \geq 0$ and that $i(0,t) \approx 0$ (i.e. dynamics occur far from the boundary).

The mean virulence, $\langle\alpha\rangle$, is given by

$$\langle\alpha\rangle = \frac{\int_0^\infty \alpha i(\alpha,t)\,d\alpha}{\int_0^\infty i(\alpha,t)\,d\alpha},$$

and hence it's time derivative is

$$\begin{aligned}\frac{d\langle\alpha\rangle}{dt} &= \frac{\int_0^\infty \alpha \frac{\partial i}{\partial t}\, d\alpha}{\int_0^\infty i(\alpha,t)\, d\alpha} - \frac{\int_0^\infty \alpha i(\alpha,t)\, d\alpha}{\left[\int_0^\infty i(\alpha,t)\, d\alpha\right]^2} \int_0^\infty \frac{\partial i}{\partial t}\, d\alpha \\ &= \frac{\int_0^\infty (\alpha - \langle\alpha\rangle) \frac{\partial i}{\partial t}\, d\alpha}{\int_0^\infty i(\alpha,t)\, d\alpha}.\end{aligned}$$

We now substitute $\partial i/\partial t$ for the expression in (1b) and simplify in order to obtain

$$\frac{d\langle\alpha\rangle}{dt} = S(t)\left\langle(\alpha - \langle\alpha\rangle)\beta(\alpha,t)\right\rangle - \sigma_\alpha^2(t), \tag{36}$$

where $\sigma_\alpha^2 = \langle\alpha^2\rangle - \langle\alpha\rangle^2$ is the variance of the virulence in the infectious population. We can now also take a Taylor expansion of $\beta(\alpha,t)$ about $\langle\alpha\rangle$ to second order in $\alpha$,

$$\begin{aligned}\left\langle(\alpha - \langle\alpha\rangle)\beta(\alpha,t)\right\rangle &= \left\langle (\alpha - \langle\alpha\rangle)\beta(\langle\alpha\rangle,t) + (\alpha - \langle\alpha\rangle)^2\beta_\alpha(\langle\alpha\rangle,t) + \frac{1}{2}(\alpha - \langle\alpha\rangle)^3\beta_{\alpha\alpha}(\langle\alpha\rangle,t)\right\rangle \\ &= \sigma_\alpha^2\beta_\alpha(\langle\alpha\rangle,t),\end{aligned}$$

where the $(\alpha - \langle\alpha\rangle)^3$ term averages to zero since we have assumed normality (normal distributions have no skew). Therefore, the equation for the time evolution of $\langle\alpha\rangle$ is

$$\frac{d\langle\alpha\rangle}{dt} = \sigma_\alpha^2\left[S\beta_\alpha(\langle\alpha\rangle,t) - 1\right], \tag{37}$$

as stated in (5c).

The time evolution for the variance is derived in a similar fashion. First note that, similar to the time derivative of $\langle\alpha\rangle$,

$$\frac{d\langle\alpha^2\rangle}{dt} = \frac{\int_0^\infty \left(\alpha^2 - \langle\alpha^2\rangle\right)\frac{\partial i}{\partial t}\, d\alpha}{\int_0^\infty i(\alpha,t)\, d\alpha},$$

which, upon substitution of (1b), simplifies to

$$\frac{d\langle\alpha^2\rangle}{dt} = S(t)\left\langle\left(\alpha^2 - \langle\alpha^2\rangle\right)\beta(\alpha,t)\right\rangle - \langle\alpha^3\rangle + \langle\alpha\rangle\langle\alpha^2\rangle + 2D.$$

This result allows us to easily compute the time derivative of $\sigma_\alpha^2$,

$$\begin{aligned}\frac{d\sigma_\alpha^2}{dt} &= \frac{d\langle\alpha^2\rangle}{dt} - 2\langle\alpha\rangle\frac{d\langle\alpha\rangle}{dt} \\ &= S(t)\left\langle\left(\alpha^2 - \langle\alpha^2\rangle\right)\beta(\alpha,t)\right\rangle - \langle\alpha^3\rangle + \langle\alpha\rangle\langle\alpha^2\rangle + 2D - 2\langle\alpha\rangle S(t)\left\langle(\alpha - \langle\alpha\rangle)\beta(\alpha,t)\right\rangle + 2\langle\alpha\rangle\sigma_\alpha^2(t) \\ &= S(t)\left\langle\left(\alpha^2 - \langle\alpha^2\rangle - 2\langle\alpha\rangle\alpha + 2\langle\alpha\rangle^2\right)\beta(\alpha,t)\right\rangle - \left(\langle\alpha^3\rangle - 3\langle\alpha\rangle\langle\alpha^2\rangle + 2\langle\alpha\rangle^3\right) + 2D \\ &= S(t)\left\langle(\alpha - \langle\alpha\rangle)^2\beta(\alpha,t)\right\rangle - S(t)\sigma_\alpha^2\langle\beta(\alpha,t)\rangle - \left(\langle\alpha^3\rangle - 3\langle\alpha\rangle\langle\alpha^2\rangle + 2\langle\alpha\rangle^3\right) + 2D.\end{aligned}$$

The term in brackets is the third cumulant of the infectious distribution and therefore is zero under our assumption of normality. We again expand $\beta(\alpha,t)$ to second order in $\alpha$. From this we obtain

$$\frac{d\sigma_\alpha^2}{dt} = \frac{1}{2}S(t)\beta_{\alpha\alpha}(\langle\alpha\rangle,t)\left(\left\langle(\alpha - \langle\alpha\rangle)^4\right\rangle - \left(\sigma_\alpha^2\right)^2\right) + 2D.$$

Finally we use the fact that the fourth central moment is equal to the sum of the fourth cumulant (which again is zero by the assumption of normality) and three times the variance squared. This gives the result quoted in (5d),

$$\frac{d\sigma_\alpha^2}{dt} = \left[\sigma_\alpha^2\right]^2 S\beta_{\alpha\alpha}(\langle\alpha\rangle,t) + 2D. \tag{38}$$

Equations (5a) and (5b) are obtained directly from the full model defined in (1) by simply expanding $\beta(\alpha,t)$ to second order as in the above two cases.